

1 **Efficacy of a patient isolation hood in reducing exposure to airborne** 2 **infectious virus in a simulated healthcare setting**

3 **Authors and Affiliations**

4 Leo Yi Yang Lee¹, Shane A Landry², Milan Jamriska³, Dinesh Subedi⁴, Simon A Joosten^{4,5,6,7}, Jeremy J
5 Barr⁴, Reece Brown³, Kevin Kevin,⁸ Robyn Schofield,⁹ Jason Monty,⁸ Kanta Subbarao^{1, 10}, Forbes
6 McGain^{11,12,13}

- 7 1. Department of Microbiology and Immunology, University of Melbourne, at The Peter Doherty
8 Institute for Infection and Immunity, Melbourne, VIC, Australia
- 9 2. Department of Physiology, School of Biomedical Sciences & Biomedical Discovery Institute,
10 Monash University, Melbourne, VIC, Australia
- 11 3. Defence Science and Technology Group, Fishermans Bend, VIC, Australia
- 12 4. School of Biological Sciences, Monash University, Clayton, VIC, Australia
- 13 5. Monash Lung, Sleep, Allergy and Immunology, Monash Health, Clayton, VIC, Australia
- 14 6. School of Clinical Sciences, Monash University, Melbourne, VIC, Australia
- 15 7. Monash Partners, Epworth, Victoria, VIC, Australia
- 16 8. School of Mechanical Engineering, University of Melbourne, Melbourne VIC, Australia.
- 17 9. School of Geography, Earth and Atmospheric Sciences, University of Melbourne, Melbourne,
18 VIC., Australia.
- 19 10. WHO Collaborating Centre for Reference and Research on Influenza, Victorian Infectious
20 Diseases Reference Laboratory at The Peter Doherty Institute for Infection and Immunity,
21 Melbourne, VIC, Australia
- 22 11. Depts. of Anaesthesia and Intensive Care, Western Health, Melbourne, VIC, Australia.
- 23 12. Dept. of Critical Care, University of Melbourne, Melbourne, VIC, Australia.

24 13. School of Public Health, University of Sydney, Sydney, NSW, Australia.

25 **Corresponding author:** Dr. Forbes McGain (footnotes)

26 **Running title:** Patient isolation hood reduces airborne virus

27 **Abstract word count:** 195

28 **Main text word count:** 2875

29 **Figures:** 5

30 **Tables:** 1

31 **Abstract**

32 **Background:** Healthcare workers treating patients with SARS-CoV-2 are at risk of infection from
33 patient-emitted virus-laden aerosols. We quantified the reduction of airborne infectious virus in a
34 simulated hospital room when a ventilated patient isolation (McMonty) hood was in use.

35 **Methods:** We nebulised 10^9 plaque forming units (PFU) of bacteriophage PhiX174 virus into a 35.1m^3
36 room with a hood active or inactive. The airborne concentration of infectious virus was measured by
37 BioSpot-VIVAS and settle plates using plaque assay quantification on the bacterial host *Escherichia coli*
38 *C*. The particle number concentration (PNC) was monitored continuously using an optical particle sizer.

39 **Results:** Median airborne viral concentration in the room reached $1.41 \times 10^5 \text{ PFU.m}^{-3}$ with the hood
40 inactive. Using the active hood as source containment reduced infectious virus concentration by 374-fold
41 in air samples. This was associated with a 109-fold reduction in total airborne particle number escape rate.
42 The deposition of infectious virus on the surface of settle plates was reduced by 87-fold.

43 **Conclusions:** The isolation hood significantly reduced airborne infectious virus exposure in a simulated
44 hospital room. Our findings support the use of the hood to limit exposure of healthcare workers to
45 airborne virus in clinical environments.

46 **Key words:** airborne infection, virus transmission, health care workers,
47 bacteriophage, aerosol science, nosocomial infection, infection control

48 **Lay summary**

49 COVID-19 patients exhale aerosol particles which can potentially carry infectious viruses into the
50 hospital environment, putting healthcare workers at risk of infection. This risk can be reduced by proper
51 use of personal protective equipment (PPE) to protect workers from virus exposure. More effective
52 strategies, however, aim to provide source control, reducing the amount of virus-contaminated air that is
53 exhaled into the hospital room.

54 The McMonty isolation hood has been developed to trap and decontaminate the air around an infected
55 patient. We tested the efficacy of the hood using a live virus model to mimic a COVID-19 patient in a
56 hospital room. Using the McMonty hood reduced the amount of exhaled air particles in the room by over
57 109-times. In our tests, people working in the room were exposed to 374-times less infectious virus in the
58 air, and room surfaces were 87-times less contaminated. Our study supports using devices like the
59 McMonty hood in combination with PPE to keep healthcare workers safe from virus exposure at work.

60 **Word count: 166**

61 **Background**

62 The treatment of patients with COVID-19 has led to considerable risk of infection in healthcare workers
63 (HCW) with associated morbidity and mortality [1, 2]. SARS-CoV-2 virus can be spread by fomites,
64 droplets and aerosol particles [2, 3]. The U.S. National Institute for Occupational Safety and Health
65 (NIOSH) hierarchy of hazard controls ranks engineering approaches to isolate people from the source of
66 risk above personal protective equipment (PPE) as methods to reduce exposure risks [4]. Nevertheless,
67 much focus has been placed upon correct PPE use by HCW (e.g. N95 mask and barrier gown wearing) in
68 lieu of improved engineering controls to reduce cross-infection of SARS-CoV-2 to HCWs and other
69 patients [3].

70 Hospital environmental engineering controls primarily rely upon negative pressure rooms (NPRs) to limit
71 the spread of airborne viruses outside of designated areas. However, NPRs are a scarce resource, may not
72 fully contain SARS-CoV-2, and importantly, may not entirely protect HCWs within the NPR [5]. Another
73 engineering control that is gaining traction is the use of portable air cleaners to enhance clearance of
74 contaminated air around HCWs, which can be used in concert with existing measures [6, 7]. It would be
75 ideal to directly control the emission source of infectious aerosols to reduce the transmission risk.

76 However, there are limited methods to contain the respiratory aerosols emitted by infectious patients, e.g.
77 placing an N95 mask on the patient, which cannot be done without compromising their care. Prior to the
78 COVID-19 pandemic, personal isolation hoods were rarely used for respiratory virus outbreaks [8],
79 although interest has recently increased [9, 10]. Several members of our research group have developed a
80 personal isolation hood (McMonty hood) [11] and examined its utility in reducing exposure to physical
81 aerosols by at least 98% in a clinical test environment [12]. Subsequently this isolation hood has been
82 adopted by many hospitals in metropolitan and regional Australia.

83 The efficacy of the isolation hood in reducing airborne viral load has not been validated, and the claimed
84 efficacy was simply derived from the reduction in the physical aerosol counts. Ideally we would have
85 tested the isolation hood's effectiveness in containing SARS-CoV-2 directly in a hospital. However, such

86 a clinical approach: (i) would have exposed research staff to patients with COVID-19; (ii) would not be
87 controlled (i.e. there would be considerable variability in aerosol emission between different patients),
88 and; (iii) would be less likely to ‘stress’ the isolation hood to prolonged worst-case scenarios with a
89 maximum number of viruses for extended durations.

90 The bacteriophage PhiX174 (family *Microviridae*) is a small (25nm, approx. ¼ SARS-CoV-2’s size) [13],
91 non-enveloped, bacteriophage with a linear ssDNA genome that is harmless to humans and is routinely
92 used as a surrogate pathogen for the study of airborne viral transmission [14-16]. Landry et al. [17]
93 recently quantified viable airborne PhiX174 virus propagated from a positive airway pressure circuit leak.
94 Nebulised viral aerosols were successfully contained by a makeshift plastic hood cover and a commercial
95 HEPA filter with a fan [17]. We aimed to test how effectively the McMonty patient isolation hood could
96 actively contain an airborne virus emission source by nebulisation of the surrogate virus PhiX174,
97 simulating the hood’s ability to limit the risk of infectious aerosol exposure to HCWs in clinical settings
98 [18].

99 **Methods**

100 Ethics approval for this laboratory-based study was deemed not required by Monash University's School
101 of Biological Sciences Ethics Manager.

102 ***Bacteriophage propagation and quantification***

103 Bacteriophage PhiX174 was propagated on its bacterial host *Escherichia coli* C (ATCC13706) grown in
104 lysogeny broth (LB). Viral product was purified from lysate using the Phage-on-Tap protocol [19] and re-
105 suspended in 1X phosphate-buffered saline (PBS, Omnipur,® Merck, Gibbstown, NJ, USA). The viable
106 concentration of PhiX174 virus stocks was quantitated by plaque assay using the soft agar overlay method
107 [19]. Viable counts of PhiX174 were expressed as plaque forming units per millilitre of suspension
108 (PFU/mL).

109 ***Patient isolation hood***

110 The McMonty isolation hood consists of a mobile steel frame, a plastic canopy, and an extraction fan
111 equipped with a standard high efficiency particulate air (HEPA) H13 filter (rated to 99.95% clearance of
112 0.3 µm particles). The plastic barrier opens out to form a hood with 1.3m³ internal volume, enclosing the
113 patient's torso from the waist up (non-airtight seal) (Figure 1). The extraction fan (Westaflex, Melbourne,
114 Australia) is mounted behind and above the patient's head. It draws the air from around the patient,
115 passing it through a HEPA filter (Techtronic Industries, Hong Kong, China) before recirculating clean air
116 to the surroundings (clean air delivery rate: CADR, at 144m³/h) [12].

117 ***Simulation of airborne virus containment using the McMonty hood in a hospital room***

118 The McMonty isolation hood was tested in a simulated hospital room that contained a single bed with the
119 hood positioned to isolate a simulated patient. PhiX174 bacteriophage was aerosolised into the sealed
120 room (4m x 3.5m x 2.4m, 35m³ internal volume) to mimic the shedding of airborne virus. The virus
121 emission source was simulated using a nebuliser (Pari-PEP®, PARI Respiratory Equipment, VA, USA)
122 placed where the head of the patient would rest (20cm above surface of bed, see Figure 2 location N) with

123 the outlet facing upwards. The Pari-PEP device produces aerosol particles with unimodal polydisperse
124 size distribution with the mass median diameter of $3.42 \pm 0.15 \mu\text{m}$ [20]. The room ventilation ports were
125 covered to avoid viral egress (i.e., no active HVAC). Sampling devices were arranged around the room to
126 detect the spread of airborne particles laden with PhiX174 (Figure 2). Room temperature and relative
127 humidity during all experiments was monitored continuously and was in the range of 21.6-27°C (mean
128 24.7°C) and 46-67% (mean 53.1%), respectively.

129 Aerosol generation experiments were conducted four times each day over three independent days during
130 July-September 2021. For each experiment, 10mL of PhiX174 virus suspension was completely nebulised
131 (airflow at 9 litres per minute, lpm) for a 40 min period. In parallel, all virus and aerosol sampling devices
132 were exposed to the air in the room for the duration. Experiment conditions were: (i) McMonty hood
133 providing active source containment, where the plastic barrier was deployed with the fan running to
134 enclose the nebuliser; or (ii) hood inactive (no containment), where the fan and plastic barrier were not
135 deployed and the nebuliser was exposed to the room. Following each nebulisation period, the room air
136 was purged of aerosols by running a portable air purifier (IQAir HealthPro 250, Goldach, Switzerland) for
137 30 mins at a CADR of 470 m³/h before beginning the next experiment.

138 ***Detection of airborne infectious PhiX174***

139 We employed the passive settle plate detection method for nebulised PhiX174 established previously by
140 Landry et al. [17] Thirteen settle plates were positioned in the room and exposed during each simulation
141 (Figure 2) to detect the deposition of airborne particles laden with infectious virus.

142 In parallel, the BioSpot-VIVAS 300-P (VIVAS; Aerosol Devices, Fort Collins, CO, USA) was used to
143 actively sample particles from air in the room at 8 lpm. The VIVAS was positioned adjacent to the
144 hospital bed and its air sample intake was located 1-2m away from the nebuliser (Figure 2). Each air
145 sample was collected as a condensed fluid into a petri dish (35mm diameter) containing 3 mL of sterile
146 PBS, which was stored at 4°C until analysis. The infectious titre of PhiX174 in VIVAS sample fluid was
147 determined by plaque assay on soft agar overlay plates of *E. coli* C as described above. VIVAS detection

148 of airborne virus was expressed as PFU per cubic metre of indoor air collected during the 40 min
149 nebulisation period (PFU.m⁻³). The VIVAS inlet and sampling lines were decontaminated
150 (Supplementary Figure S2) by flushing with 70% ethanol then distilled water prior to the next sample.

151 *Aerosol monitoring instrumentation*

152 Airborne particle number distribution and concentration were monitored during each experiment using an
153 optical particle sizer (OPS, TSI Model 3300), which allows detection and size classification of aerosol
154 particles within a 0.3–10µm diameter range. McMonty hood performance was assessed using total
155 particle number concentration (PNC). The instrument was placed outside of the hood at the foot of the
156 patient bed with sampling inlet 0.2m above the bed (Figure 2) and logged measurements at 10 second
157 average intervals. The OPS was present for two out of three independent experimental days
158 (Supplementary Materials).

159 *Data analysis*

160 Infectious phage samples from each experiment were categorised based on their relative exposure to the
161 nebuliser with the McMonty hood active or inactive. Data from all simulation samples were treated as
162 experimental replicates and pooled according to containment condition. Settle plates counts exceeding the
163 limit of detection were included as 300 PFU. The untransformed PFU counts (settle plate) or PFU.m⁻³
164 (VIVAS) were compared between each containment condition by the Wilcoxon rank sum test (R version
165 4.1.1, The R Foundation for Statistical Computing, Vienna; package ‘rstatix’). P values <0.05 were
166 considered statistically significant. Wilcoxon effect size (r) was calculated as Z score/√(sample size). For
167 both settle plate and VIVAS data, we compared the fold-change in median values for McMonty hood
168 active versus inactive datasets to express the reduction in bacteriophage resulting from the use of active
169 source containment.

170 We defined a theoretical model to describe the PNC inside the room throughout each experiment
171 (Supplementary Materials). The model explains rate of change in PNC over time (per minute) through a

172 combination of (i) the number of viral aerosol particles escaping the hood; and (ii) the number of viral
173 aerosol particles in the room lost through deposition. Experimental PNC data measured by the OPS was
174 fitted to this model to calculate the number of particles escaping into the room when the McMonty hood
175 was active versus inactive. These values were used to calculate the effective filtration efficiency,
176 expressed as the percentage (%) of particles the hood prevents from escaping into the room.

177 **Results**

178 *Patient isolation using the McMonty hood reduces concentration of airborne infectious virus*

179 Figure 3 shows the airborne concentration of infectious PhiX174 in the room using an active McMonty
180 hood compared to an inactive control condition (no containment). With active containment of the
181 emission source, the median concentration of viable virus in air samples was 3.77×10^2 PFU.m⁻³ (n=6,
182 IQR=262-1,277) compared to 1.41×10^5 PFU.m⁻³ (n=7, IQR=33,750-182,500) without containment. This
183 equates to a significant 374-fold reduction in airborne infectious virus contamination (W=0, p<0.005,
184 r=0.83).

185 *Effect of the Active McMonty hood upon containment of airborne particles*

186 Airborne particle number concentrations (PNCs) for McMonty active and inactive no containment
187 conditions are shown in Figure 4. Both datasets were fitted to a model (Supplementary Materials) to
188 quantify the rate of viral aerosol escaping into the simulation room in each case. One room simulation
189 with the McMonty hood active was excluded from analysis due to data inconsistencies (Supplementary
190 Figure S1).

191 The combined PNC data for each condition show clear common trends and limited variability, indicating
192 good reproducibility between each experiment. Furthermore, the fitted model shows good agreement with
193 both datasets, with adjusted r^2 values of 0.86 when the McMonty Hood is active and 0.96 when inactive.

194 A clear 2 orders of magnitude decrease in PNC was observed within the room when the McMonty hood is
195 active (Figure 4). This large reduction was also reflected in the modelled escape rates (Table 1) with a
196 109 ± 5 fold reduction in the rate of viral aerosol escape into the room when the hood is active. Effective
197 filtration efficiency of the hood (calculations in supplement) indicated that the active McMonty hood
198 successfully removed 99.1 ± 0.1 % of viral aerosol released. Comparing total airborne particle (via OPS)
199 and infectious airborne virus (via VIVAS) measurements shows that active McMonty hood containment
200 mitigates >99% of respiratory exposure in our simulated hospital room.

201 **Table 1. Summary of physical and infectious aerosol results from OPS and VIVAS.** Fitted values of
 202 viral aerosol escape rates (\pm mean standard deviations) with the McMonty hood active or inactive are
 203 presented, with the calculated fold reduction and effective filtration efficiency. Median virus
 204 concentration (\pm median absolute deviation) measurements are provided for VIVAS virological data;
 205 corresponding fold reduction and percentage reductions are calculated from the median values.

Physical Aerosol Analysis	McMonty Active Escape Rate ($\log_{10}\#\cdot\text{min}^{-1}$)	Inactive (No Containment) Escape Rate ($\log_{10}\#\cdot\text{min}^{-1}$)	Fold Reduction	Effective Filtration Efficiency (%)
	7.99 \pm 6.60	10.02 \pm 8.48	109 \pm 5	99.1 \pm 0.1
Virological Aerosol Analysis	McMonty Active Viral Conc. (median) ($\log_{10}\text{PFU}\cdot\text{m}^{-3}$)	Inactive Viral Conc. (median) ($\log_{10}\text{PFU}\cdot\text{m}^{-3}$)	Fold Reduction	Percentage Reduction (%)
	2.58 \pm 2.36	5.15 \pm 5.14	374	99.7

206

207 ***Infectious virus counts from airborne particles which deposited onto the surface of settle***
 208 ***plates***

209 Infectious virus counts on settle plates were reduced with active source containment (<11 PFU), and
 210 33/108 plates did not detect any viable phage. Active isolation hood containment significantly reduced the
 211 median settle plate count (median=2, n=108 IQR=0-4) by 87-fold (W=91.5, p<0.001, r=0.775) compared
 212 to plates without source containment (median=174, n=48, IQR=94.5-300) (Figure 5).

213 **Discussion**

214 In a simulated patient room, we nebulised a high titre bacteriophage (PhiX174) suspension, comparing
215 infectious phage numbers and particle number concentrations (PNCs) when a McMonty isolation hood
216 was active/inactive. Measurements of virus-laden aerosols using the Bio-Spot VIVAS showed a 374-fold
217 reduction in infectious virus concentration, and a 109-fold reduction in particle escape rates when the
218 isolation hood was active. That is, viral aerosol spread was reduced by >99% when the isolation hood was
219 active, consistent with our prior study using non-infectious aerosols [12]. There was also an 87-fold
220 reduction in viable virus deposited onto bacterial settle plates when the hood was active, indicating a
221 reduced risk of contamination of surfaces.

222 Nielsen et al. [8] in 2009 discussed the utility of personalized ventilation as part of a suite of indoor
223 controls of airborne infectious diseases. Johnson et al. (2009) found that effective isolation was possible
224 using feasible, low-technology, low-cost structures readily constructed within hospitals in emergency
225 situations [21]. Since the COVID-19 pandemic several groups have focused upon aerosol containment at
226 the point of emission with personal isolation units, including ventilated headboards [9], and similar
227 stationary devices [10] attached to building ventilation units. Nishimura et al. atomised influenza virus
228 inside their Barrihood isolation fan/filter unit, finding that none escaped [22]. Using a bacteriophage
229 model similar to our study, Landry et al. (2022b) showed that a makeshift isolation hood greatly
230 augments the protection conferred by standard hospital PPE by limiting skin exposure to viral aerosols
231 [23]. Despite the success of these isolation hood concepts in experimental settings, such devices have not
232 been in widespread use by HCWs during the COVID-19 pandemic.

233 Concessions to human comfort requirements must be addressed for the adoption of isolation hoods in
234 clinical settings. Correlating well with our previous report using non-infectious aerosols [12], we found
235 that the McMonty hood achieved a 99.1% effective filtration efficiency by aerosol particle counts. This
236 was lower than the theoretical 99.95% filtration efficiency of its H13 HEPA unit [12], indicating that the

237 small fraction of viral aerosol escaping the hood was likely diffusing underneath the hood skirting rather
238 than penetrating through the exhaust filter. This trade-off aims to improve patient comfort and usability
239 by maintaining lower (<0.5 m/s) airflow rates near the patient [24], while cognisant that lower air flow
240 rates reduce the efficacy of clearing infectious respiratory agents.

241 Our study has some limitations. First, while the bacteriophage PhiX174 is a safe surrogate for airborne
242 viral spread, it is unenveloped, unlike coronaviruses and influenza viruses, which may affect its
243 environmental stability [17]. Second, we analysed airborne and settle plate viral contamination in a
244 laboratory room that simulates a functionally uniform aerial viral distribution, in the absence of either
245 active HVAC or air mixing. Similarly, the concentrated viral inoculum nebulised into our simulation
246 room was several orders of magnitude higher than previously reported levels of airborne infectious virus
247 shed by COVID-19 patients [25-27]. The detection of approx. 10^3 PFU.m⁻³ airborne phage escaping hood
248 containment is likely a result of this amplified viral challenge. Combined, these environmental and viral
249 load factors produce an extreme test scenario. Finally, we used a nebuliser which produces a relatively
250 narrow range of particle sizes (aerosol mass median diameter $3.42 \pm 0.15\mu\text{m}$) to produce virus-laden
251 aerosols. Human generated aerosols are of similar mean size [28], though with a broader size distribution,
252 particularly for large, visible droplets [29].

253 We employed two methods to quantitate infectious airborne virus levels to address different types of
254 exposure risk. Bacteriophage counts from the VIVAS were approximately 100-fold higher than floor
255 settle plates, as the device actively pumps large air volumes to capture suspended infectious aerosols into
256 a liquid sample. In contrast, the bacterial plates relied on passive deposition of aerosols onto <1% of the
257 floor surface area, thus high viral loads/concentrations were required to account for this difference in
258 sensitivity [17]. The VIVAS may have further reduced the sensitivity of the plate counts by competition
259 as it was drawing in virus-laden air away from the plates. These sampling techniques can be correlated to
260 different risk factors in a hospital environment involving airborne viral contamination. The respiratory
261 exposure risk of medical staff in virus-infected patient rooms can be approximated by the VIVAS air

262 sampling rate of 8 lpm, which is similar to human minute ventilation rates (7 lpm) [30]. The deposition of
263 infectious virus aerosols onto the surface of settle plates can similarly relate to the potential risk of fomite
264 generation on contaminated room surfaces, although our experimental setting lacked realistic airflow by
265 HVAC. In our test system, the McMonty hood substantially reduced viral exposure by both these metrics.

266 We have shown that a personal isolation hood can effectively reduce viral and aerosol escape by >99% in
267 a simulated indoor healthcare setting. Along with our recent clinical study of ease-of-use [31], these
268 findings support the clinical use of the hood to limit HCW exposure to airborne virus. Complementary
269 efforts to clean indoor air environments with HEPA filtered air cleaners in hospitals [6, 7] and beyond are
270 also useful to prevent respiratory infections. Undertaking a randomised, controlled clinical trial of the
271 efficacy of isolation hoods (or of air cleaners) in preventing HCW SARS-CoV-2 infections is likely to be
272 overwhelmingly challenging due to the large sample size required.

273 **References**

- 274 1. Bandyopadhyay S, Baticulon RE, Kadhum M, et al. Infection and mortality of healthcare workers
275 worldwide from COVID-19: a systematic review. *BMJ global health* **2020**; 5:e003097.
- 276 2. World Health Organization. Transmission of SARS-CoV-2: implications for infection prevention
277 precautions. Available at: [https://www.who.int/news-room/commentaries/detail/transmission-of-sars-cov-](https://www.who.int/news-room/commentaries/detail/transmission-of-sars-cov-2-implications-for-infection-prevention-precautions)
278 [2-implications-for-infection-prevention-precautions](https://www.who.int/news-room/commentaries/detail/transmission-of-sars-cov-2-implications-for-infection-prevention-precautions).
- 279 3. Morawska L, Cao J. Airborne transmission of SARS-CoV-2: the world should face the reality.
280 *Environment International* **2020**; 2020 Apr 10;139:105730. doi: 10.1016/j.envint.2020.105730:105730.
- 281 4. (NIOSH) TNIfOSaH. Hierarchy of Controls. Available at:
282 <https://www.cdc.gov/niosh/topics/hierarchy/default.html>.
- 283 5. Santarpia JL, Rivera DN, Herrera VL, et al. Aerosol and surface contamination of SARS-CoV-2
284 observed in quarantine and isolation care. *Scientific reports* **2020**; 10:1-8.
- 285 6. Busing KL, Schofield R, Irving L, et al. Use of portable air cleaners to reduce aerosol transmission on
286 a hospital COVID-19 ward. *medRxiv* **2021**.
- 287 7. Landry SA, Subedi D, Barr JJ, et al. Fit-tested N95 masks combined with portable HEPA filtration can
288 protect against high aerosolized viral loads over prolonged periods at close range. *The Journal of*
289 *Infectious Diseases* **2022a**.
- 290 8. Nielsen PV. Control of airborne infectious diseases in ventilated spaces. *Journal of the Royal Society*
291 *Interface* **2009**; 6:S747-S55.
- 292 9. Centers for Disease Control and Prevention. NIOSH Ventilated Headboard Provides Solution to Patient
293 Isolation During an Epidemic. Available at: [https://blogs.cdc.gov/niosh-science-](https://blogs.cdc.gov/niosh-science-blog/2020/04/14/ventilated-headboard/?deliveryName=USCDC-170-DM25875)
294 [blog/2020/04/14/ventilated-headboard/?deliveryName=USCDC-170-DM25875](https://blogs.cdc.gov/niosh-science-blog/2020/04/14/ventilated-headboard/?deliveryName=USCDC-170-DM25875).
- 295 10. Adir Y, Segol O, Kompaniets D, et al. Covid19: minimising risk to healthcare workers during aerosol
296 producing respiratory therapy using an innovative constant flow canopy. *European Respiratory Journal*
297 **2020**; 55:2001017.

- 298 11. Medihood. The McMonty Medihood. Available at: <https://medihood.com.au/>.
- 299 12. McGain F, Humphries RS, Lee JH, et al. Aerosol generation related to respiratory interventions and
300 the effectiveness of a personal ventilation hood. *Crit Care Resusc* **2020**.
- 301 13. Bar-On YM, Flamholz A, Phillips R, Milo R. SARS-CoV-2 (COVID-19) by the numbers. *Elife* **2020**;
302 9:e57309.
- 303 14. Verreault D, Moineau S, Duchaine C. Methods for sampling of airborne viruses. *Microbiology and*
304 *molecular biology reviews* **2008**; 72:413-44.
- 305 15. Turgeon N, Toulouse M-J, Martel B, Moineau S, Duchaine C. Comparison of five bacteriophages as
306 models for viral aerosol studies. *Applied and environmental microbiology* **2014**; 80:4242-50.
- 307 16. Kumar S, Nyodu R, Maurya VK, Saxena SK. Morphology, Genome Organization, Replication, and
308 Pathogenesis of Severe Acute Respiratory Syndrome Coronavirus 2 (SARS-CoV-2). *Coronavirus Disease*
309 *2019 (COVID-19)* **2020**:23-31.
- 310 17. Landry SA, Barr JJ, MacDonald MI, et al. Viable virus aerosol propagation by positive airway
311 pressure (PAP) circuit leak and mitigation with a ventilated patient hood. *European Respiratory Journal*
312 **2020**.
- 313 18. Tran K, Cimon K, Severn M, Pessoa-Silva CL, Conly J. Aerosol generating procedures and risk of
314 transmission of acute respiratory infections to healthcare workers: a systematic review. *PLoS One* **2012**;
315 7:e35797.
- 316 19. Bonilla N, Rojas MI, Cruz GNF, Hung S-H, Rohwer F, Barr JJ. Phage on tap—a quick and efficient
317 protocol for the preparation of bacteriophage laboratory stocks. *PeerJ* **2016**; 4:e2261.
- 318 20. Berlinski A. In vitro evaluation of positive expiratory pressure devices attached to nebulizers.
319 *Respiratory care* **2014**; 59:216-22.
- 320 21. Johnson DL, Lynch RA, Mead KR. Containment effectiveness of expedient patient isolation units.
321 *American journal of infection control* **2009**; 37:94-100.
- 322 22. Nishimura H, Fan Y, Sakata S. New applications of a portable isolation hood for use in several
323 settings and as a clean hood. *Journal of Thoracic Disease* **2020**; 12:3500.

- 324 23. Landry SA, Subedi D, MacDonald MI, et al. Point of emission air filtration enhances protection of
325 healthcare workers against skin contamination with virus aerosol. *Respirology* **2022b**.
- 326 24. FANGER PO, Christensen N. Perception of draught in ventilated spaces. *Ergonomics* **1986**; 29:215-
327 35.
- 328 25. Lednicky JA, Lauzard M, Fan ZH, et al. Viable SARS-CoV-2 in the air of a hospital room with
329 COVID-19 patients. *International journal of infectious diseases : IJID : official publication of the*
330 *International Society for Infectious Diseases* **2020**; 100:476-82.
- 331 26. Leung NH, Chu DK, Shiu EY, et al. Respiratory virus shedding in exhaled breath and efficacy of face
332 masks. *Nature Medicine* **2020**:1-5.
- 333 27. Coleman KK, Tay DJW, Tan KS, et al. Viral load of severe acute respiratory syndrome coronavirus 2
334 (SARS-CoV-2) in respiratory aerosols emitted by patients with coronavirus disease 2019 (COVID-19)
335 while breathing, talking, and singing. *Clinical Infectious Diseases* **2021**.
- 336 28. Johnson G, Morawska L, Ristovski Z, et al. Modality of human expired aerosol size distributions.
337 *Journal of Aerosol Science* **2011**; 42:839-51.
- 338 29. Gaeckle NT, Lee J, Park Y, Kreykes G, Evans MD, Hogan Jr CJ. Aerosol generation from the
339 respiratory tract with various modes of oxygen delivery. *American journal of respiratory and critical care*
340 *medicine* **2020**; 202:1115-24.
- 341 30. Mehta JH, Williams GW, II, Harvey BC, Grewal NK, George EE. The relationship between minute
342 ventilation and end tidal CO₂ in intubated and spontaneously breathing patients undergoing procedural
343 sedation. *PLOS ONE* **2017**; 12:e0180187.
- 344 31. McGain F, Bates S, Lee JH, et al. A prospective clinical evaluation of a patient isolation hood during
345 the COVID-19 pandemic. *Australian Critical Care* **2021**.
- 346

347 **Figure legends**

348 **Figure 1. McMonty personal isolation hood in active configuration.** Hood deployed in simulated
349 hospital room in experiment conditions. VIVAS instrument and settle plates visibly arranged around
350 mock patient bed. Photo credit: Shane Landry (from experiment monitoring camera).

351 **Figure 2. Locations of settle plates, the VIVAS machine and OPS in the simulation room.** All
352 experiments were performed in a clinical room with dimensions $4.0 \times 3.25 \times 2.7$ m (volume = 35.1 m^3)
353 containing a bed and the McMonty hood. Ten settle plates (grey circles) and three hanging plates (grey
354 triangles) were hung at head height perpendicular to the floor. The nebuliser (N, orange diamond) was
355 positioned at the head of the bed, with the exit point facing vertically upwards. Air sampling was
356 performed using a BioSpot VIVAS positioned at the bedside 1-2 m from the nebuliser. Particle
357 concentration as assessed by optical particle sizer (OPS) posited in the centre of the bed, outside the hood.
358 Virus and aerosol measurements were taken when the nebuliser was actively contained by the hood (i.e.,
359 hood physically isolated nebuliser from instruments), compared to when no containment was used (i.e.,
360 instruments were exposed to nebuliser).

361 **Figure 3. Violin-plot of viable airborne phage concentration (PFU.m^{-3}) detected by Bio-Spot VIVAS**
362 **(y-axis) in each containment condition (x-axis).** Distribution of individual measurements (black points)
363 of bacteriophage plaque forming units per m^3 of air (PFU.m^{-3}) when the McMonty hood was inactive
364 during the sampling period (blue fill) compared to measurements taken when active hood source
365 containment was used (red fill). Annotated 374-fold reduction of median airborne virus concentration
366 when McMonty hood was active. Groups were compared (untransformed values) by Wilcoxon rank sum
367 test.

368 **Figure 4. PNC data from OPS measurements taken during airborne phage experiments.** Data
369 grouped based on containment type and fitted to theoretical model with 95% confidence interval.
370 Labelled fold-reduction of particle number escape rate when McMonty hood is active (data points in red)
371 compared to inactive (data points in blue).

372 **Figure 5. Violin-plot of total viable phage count (PFU) detected on settle plates (y-axis) in each**
373 **containment condition (x-axis).** Distribution of individual plaque forming unit (PFU) counts (black
374 points) for each settle plate when no containment (inactive hood) was used during the sampling period
375 (blue fill) compared to counts reached when active McMonty hood containment was used (red fill).
376 Counts transformed by +1 PFU to visualise 0 PFU plates on the \log_{10} scale (on graph only). Plates with
377 plaque counts exceeding the saturation point on each plate were given the value of 300 for statistical tests
378 (threshold labelled as too many to count; TMTC). Annotated 87-fold reduction of median settle plate
379 count when McMonty hood is active. Groups were compared (untransformed values) by Wilcoxon rank
380 sum test, $p < 0.05$ indicates statistically significant difference. Outliers were excluded from violin-plot
381 visualisations but are visible in the scatterplot.

382 **Footnotes**

383 **Authors contributions:** LYYL, SAL, SJ, MJ, JB, KS and FM contributed to study concept and design;
384 LYYL, SAL, SJ, MJ, DS, JB, and FM contributed to acquisition of the data, LYYL, DS, RB, MJ, SAL,
385 SJ and FM contributed to data analysis and interpretation; LYYL, FM, RB, MJ, DS and JB contributed to
386 the initial drafting of the manuscript; all authors contributed to critical revision of the report.

387 **Funding Sources:** 2020 MRFF BioMedical Translation Bridge (BTBR 300182) Grant. KS is supported
388 by an NHMRC Investigator grant. The BioSpot VIVAS was purchased via a donation to the Royal
389 Melbourne Hospital. The Melbourne WHO Collaborating Centre for Reference and Research on
390 Influenza is supported by the Australian Government Department of Health.

391 **Declaration of Interests:** The University of Melbourne and Western Health have a patent for the
392 McMonty Hood. Forbes McGain and Jason Monty could receive royalties for sales of the McMonty
393 isolation hood. The manufacturers of the McMonty hood had no role in this study's design nor manuscript
394 preparation. All other authors have no conflicts of interest to declare.

395 **Corresponding author contact details:**

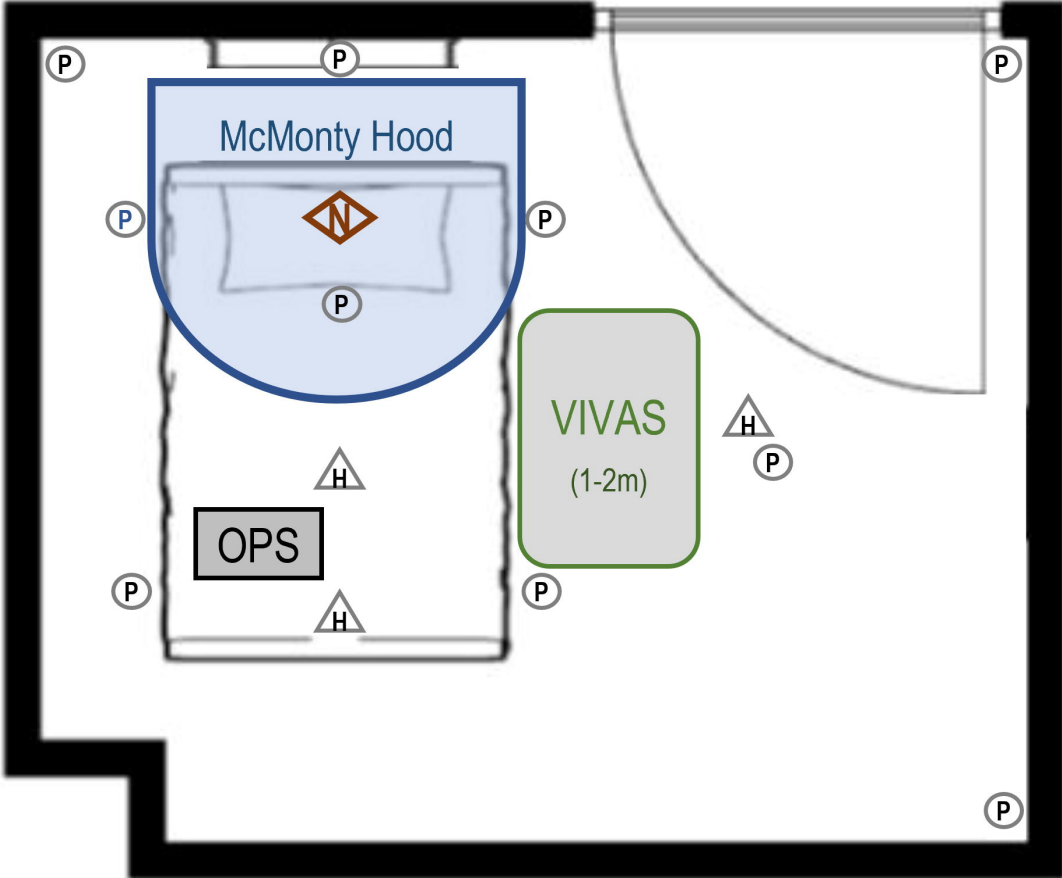
396 Dr. Forbes McGain

397 Email: forbes.mcgain@wh.org.au

398 Telephone: +61 3 8345 1333

399 Contact address: Sunshine Hospital, Furlong Road, St Albans, VIC 3021, Australia





P

P

P

McMonty Hood

P

N

P

P

VIVAS
(1-2m)

H

P

H

OPS

P

P

H

P

